Title

The maize heterotrimeric G protein β subunit controls shoot meristem development and immune responses

Journal

Proceedings of the National Academy of Sciences of the United States of America, 117(3)

ISSN

0027-8424

Authors

Wu, Qingyu
Xu, Fang
Liu, Lei
et al.

Publication Date

2020-01-21

DOI

10.1073/pnas.1917577116

Peer reviewed

The maize heterotrimeric G protein β subunit controls shoot meristem development and immune responses

Qingyu Wu[a,b,1], Fang Xu[a,c,1], Lei Liu[a], Si Nian Char[d], Yezhang Ding[e], Byoung Il Je[a,f], Eric Schmelz[e], Bing Yang[d,g], and David Jackson[a,2]

[a]Cold Spring Harbor Laboratory, Cold Spring Harbor, NY 11724; [b]Institute of Agricultural Resources and Regional Planning, Chinese Academy of Agricultural Sciences, 100081 Beijing, China; [c]Key Laboratory of Plant Development and Environmental Adaption Biology, Ministry of Education, School of Life Sciences, Shandong University, 266237 Qingdao, China; [d]Division of Plant Sciences, University of Missouri, Columbia, MO 65211; [e]Division of Biological Science, University of California San Diego, La Jolla, CA 92093; [f]Department of Horticultural Bioscience, Pusan National University, 50463 Miryang, Republic of Korea; and [g]Donald Danforth Plant Science Center, St. Louis, MO 63132

Edited by Natasha V. Raikhel, Center for Plant Cell Biology, Riverside, CA, and approved November 18, 2019 (received for review October 8, 2019)

Heterotrimeric G proteins are important transducers of receptor signaling, functioning in plants with CLAVATA receptors in controlling shoot meristem size and with pathogen-associated molecular pattern receptors in basal immunity. However, whether specific members of the heterotrimeric complex potentiate cross-talk between development and defense, and the extent to which these functions are conserved across species, have not yet been addressed. Here we used CRISPR/Cas9 to knock out the maize G protein β subunit gene (*Gβ*) and found that the mutants are lethal, differing from those in *Arabidopsis*, in which homologous mutants have normal growth and fertility. We show that lethality is caused not by a specific developmental arrest, but by autoimmunity. We used a genetic diversity screen to suppress the lethal *Gβ* phenotype and also identified a maize *Gβ* allele with weak autoimmune responses but strong development phenotypes. Using these tools, we show that *Gβ* controls meristem size in maize, acting epistatically with G protein α subunit gene (*Gα*), suggesting that *Gβ* and *Gα* function in a common signaling complex. Furthermore, we used an association study to show that natural variation in *Gβ* influences maize kernel row number, an important agronomic trait. Our results demonstrate the dual role of *Gβ* in immunity and development in a cereal crop and suggest that it functions in cross-talk between these competing signaling networks. Therefore, modification of Gβ has the potential to optimize the trade-off between growth and defense signaling to improve agronomic production.

heterotrimeric G protein | meristem | fasciation | maize | autoimmunity

Shoots are derived from meristems, pools of self-renewing stem cells that initiate new organs from their daughter cells (1). The development of the shoot apical meristem (SAM) is controlled by the CLAVATA (CLV)-WUSCHEL (WUS) feedback signaling pathway (1). This pathway includes a secreted peptide, CLV3; its leucine-rich repeat receptor-like kinase (LRR-RLK), CLV1; and a homeodomain transcription factor, WUS, which promotes *CLV* gene expression and stem cell fate (2–7). CLV1 binds and perceives the CLV3 peptide, leading to WUS repression (4, 8, 9). A second LRR protein, CLV2, is a receptor-like protein that controls meristem size in parallel to CLV1 (10, 11). The CLV-WUS feedback loop was discovered in the model species *Arabidopsis* but is conserved widely, including in cereal crops. Through characterization of maize *fasciated ear* (*fea*) mutants with enlarged inflorescence meristems (IMs), the *THICK TASSEL DWARF1* (*TD1*), *FASCIATED EAR2* (*FEA2*), and *ZmCLAVATA3/EMBRYO SURROUNDING REGION-RELATED7* (*ZmCLE7*) genes have been identified as orthologs of *CLV1*, *CLV2*, and *CLV3* respectively (12–16). In addition to the conventional CLV1 receptor, the LRR receptor-like protein FASCIATED EAR3 (FEA3) represses WUS from below and perceives a distinct CLE peptide, ZmFON2-LIKE CLE PROTEIN1 (ZmFCP1) (15). Therefore, distinct CLV receptors perceive small CLE peptides to maintain the balance of meristem proliferation and differentiation. However, the downstream signaling events from these receptors are not well understood.

Heterotrimeric G proteins, consisting of Gα, Gβ, and Gγ subunits, transduce signals downstream of receptors (17). In the standard animal model, a GDP-bound Gα associates with a Gβγ dimer and a 7-pass transmembrane (7-TM) G protein-coupled receptor (GPCR) in its inactive state. On ligand perception, the GPCR promotes GDP release and binding of GTP by Gα, activating the G proteins and promoting interaction with downstream effectors (17). However, G protein signaling in plants appears to be fundamentally different, and whether plants have 7-TM GPCRs remain under debate (18–20). In contrast, emerging evidence suggests that heterotrimeric G proteins in plants interact with single-pass transmembrane receptors (21–24). For example, the maize Gα subunit COMPACT PLANT2 (CT2) interacts with the CLV2 ortholog FEA2 to control shoot meristem development, and *ct2* mutants have enlarged SAMs and fasciated ears (21). Similarly, the *Arabidopsis* Gβ subunit (AGB1) interacts with another CLV-like receptor, RECEPTOR-LIKE PROTEIN KINASE2 (RPK2), to control *Arabidopsis* SAM development, and *Arabidopsis agb1* mutant SAMs are larger (21, 23).

In addition to their developmental functions, heterotrimeric G proteins also positively regulate plant immunity. For example, AGB1 and EXTRA-LARGE GTP-BINDING PROTEIN2 (XLG2), a noncanonical Gα in *Arabidopsis*, interact with the immune receptor

Significance

Cereal crops, such as maize, provide our major sources of food and feed. Crop productivity has been significantly improved by the selection of favorable architecture and development alleles; however, crops are constantly under attack from pathogens, which severely limits yield due to a defense–growth trade-off. Therefore, identifying key signaling regulators that control both developmental and immune signaling is critical to provide basic knowledge to maximize productivity. This work shows that the maize G protein β subunit regulates both meristem development and immune signaling and suggests that manipulation of this gene has the potential to optimize the trade-off between yield and disease resistance to improve crop yields.

Author contributions: Q.W., F.X., and D.J. designed research; Q.W., F.X., L.L., S.N.C., Y.D., B.I.J., E.S., and B.Y. performed research; Q.W., F.X., L.L., S.N.C., Y.D., E.S., B.Y., and D.J. analyzed data; and Q.W., F.X., and D.J. wrote the paper.

The authors declare no competing interest.

This article is a PNAS Direct Submission.

See online for related content such as Commentaries.

[1]Q.W. and F.X. contributed equally to this work.

[2]To whom correspondence should be addressed. Email: jacksond@cshl.edu.

This article contains supporting information online at https://www.pnas.org/lookup/suppl/doi:10.1073/pnas.1917577116/-/DCSupplemental.

First published December 18, 2019.

FLAGELLIN SENSITIVE2 (FLS2) as well as with its downstream kinase BOTRYTIS-INDUCED KINASE1 (BIK1), which is stabilized by this interaction (24), and immunity is compromised in *xlg* and *gβ* mutants (24, 25). RNAi suppression of the rice *Gβ* gene *RGB1* causes browning of internodes and ectopic cell death in roots, phenotypes associated with immune defects (26, 27). However, the functions of monocot Gβ genes in development have not been dissected, because CRISPR/Cas9-derived *rgb1* null mutants die soon after germination (28, 29).

Here we report that CRISPR/Cas9-induced knockouts of maize *Gβ* (*ZmGB1*) are seedling lethal, distinct from *Arabidopsis* but similar to rice. We found that lethality was due to autoimmunity rather than to a developmental arrest. We rescued lethality by introgressing *Zmgb1* CRISPR ($Zmgb1^{CR}$) mutants into a suppressive genetic background and found that the mutants had larger SAMs and fasciated inflorescences. We also identified a viable allele of *ZmGB1* by map-based cloning of a fasciated ear mutant, *fea*183*, which preferentially alleviated immune phenotypes. Our study dissects the dual functions of *Gβ* in shoot meristem development and immune responses, suggesting that modulation of G protein signaling has the potential to optimize the trade-off between yield and disease resistance in crop plants.

Results

Knockout of *ZmGB1* Using CRISPR/Cas9 Causes Lethality Due to Autoimmunity. Maize Gα (CT2) and *Arabidopsis* Gα and Gβ subunits control meristem development (21, 23, 30). However, the role of Gβ in meristem regulation in the grasses remains obscure, because rice *Gβ* knockouts are lethal, leading to the proposal that it is essential for growth (28, 29). To study the function of maize Gβ, we used CRISPR/Cas9 to generate multiple alleles, including 1-bp and 136-bp deletions with premature stop codons predicted to result in null alleles (Fig. 1*A*). Homozygous $Zmgb1^{CR}$ mutants germinated normally but arrested and turned yellow, then brown, and died at an early seedling stage (Fig. 1*B*).

The necrotic appearance of $Zmgb1^{CR}$ mutants, along with the known role of *AGB1* in *Arabidopsis* immune responses (24, 25), prompted us to survey immune markers. We first checked for cell death by staining with Trypan blue. $Zmgb1^{CR}$ mutants were heavily stained compared with wild-type (WT), suggesting that they were undergoing cell death (Fig. 1*C*). In support of this, 3,3′-diaminobenzidine (DAB) staining showed that H_2O_2, another marker for immune responses, accumulated in the mutants (Fig. 1*D*). We also checked the expression of 2 immune marker genes, *PATHOGENESIS-RELATED PROTEIN1* (*PR1*) and *PR5*, and found that both were significantly higher in $Zmgb1^{CR}$ mutants (Fig. 1*E*), as were levels of the defense hormone salicylic acid (Fig. 1*F*). Similar necrotic phenotypes were found in mutants grown in sterile culture, which together with the up-regulation of immune markers suggests that $Zmgb1^{CR}$ mutants died because of an autoimmune response.

To confirm that the phenotypes were due to mutation of *ZmGB1* and not to an off-target effect of CRISPR/Cas9, we made a translational fusion of the *ZmGB1* genomic sequence with YELLOW FLUORESCENT PROTEIN (YFP)-STREPTAVIDIN-BINDING PEPTIDE (SBP) at its N terminus, under the control of its native promoter and terminator. This construct was transformed into maize and backcrossed twice to $Zmgb1^{CR}$ heterozygotes in the B73 background. The YFP-SBP-ZmGB1 transgene was able to complement the lethal phenotypes of $Zmgb1^{CR}$ mutants (*SI Appendix*, Table S1). Imaging revealed YFP-SBP-ZmGB1 localization to the plasma membrane (Fig. 1*G*), as expected (31) and confirmed by colocalization with FM4-64 after plasmolysis

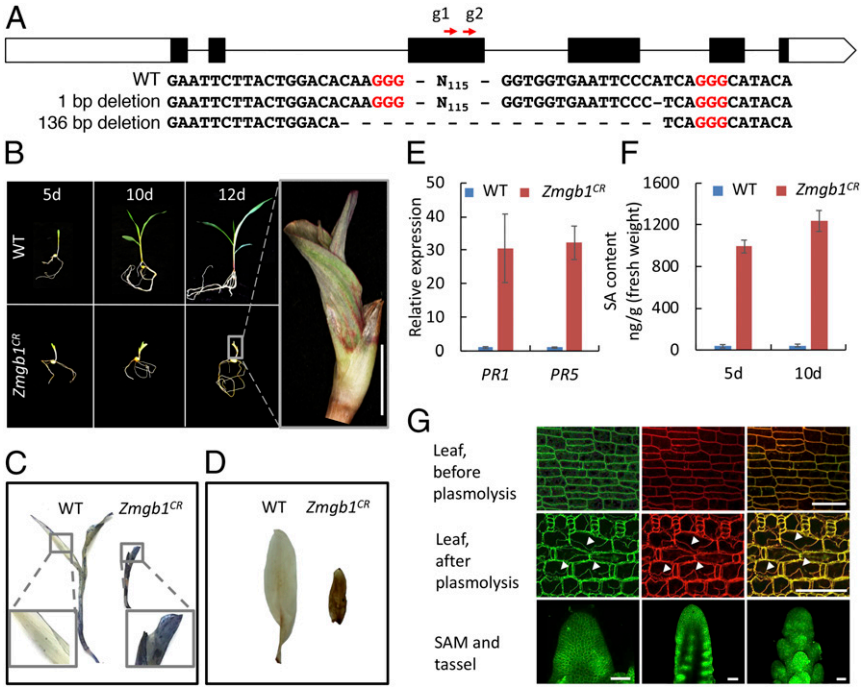

Fig. 1. CRISPR/Cas9 knockouts of *ZmGB1* led to autoimmune phenotypes. (*A*) CRISPR/Cas9 editing of *ZmGB1* produced different frameshift alleles. White boxes indicate 5′ and 3′ UTRs, black boxes indicate exons, and black lines indicate introns. The positions of guide RNAs are indicated by red arrows. (*B*) $Zmgb1^{CR}$ mutants were lethal at the seedling stage. The pictures were taken at 5, 10, and 12 d after seeds were sown in soil. (*Upper*) WT. (*Lower*) $Zmgb1^{CR}$ mutants. (Scale bar: 1 cm.) (*C* and *D*) Trypan blue (*C*) and DAB (*D*) staining of WT and $Zmgb1^{CR}$ mutants showed increased staining in the mutants. (*E*) *PR1* and *PR5* expression were up-regulated in the $Zmgb1^{CR}$ mutants, and both 5-d-old and 10-d-old $Zmgb1^{CR}$ mutants accumulated significantly more salicylic acid (SA) (*F*). For *E* and *F*, $P = 0.0001$, Student's *t* test; $n = 3$. (*G*) YFP-SBP-ZmGB1 localizes to membranes in shoot meristems. (*Upper*) Leaf cells expressing YFP-SBP-ZmGB1 (green), counterstained with FM4-64 (red), both visible as a thin line and overlapped (yellow) around the cell. (*Middle*) Following plasmolysis, YFP-SBP-ZmGB1 (arrows) remained colocalized with FM4-64. (*Lower*) YFP-SBP-ZmGB1 expression was found throughout SAM and tassel inflorescence primordia. (Scale bars: 50 μm.)

(Fig. 1*G*). Consistent with its anticipated role in shoot development, *ZmGB1* was expressed throughout the SAM and IMs (Fig. 1*G*).

Having confirmed the *Zmgb1* phenotypes, we asked why the phenotypes of *Arabidopsis Gβ* mutants (reduced immune response, but overall normal growth and fertility) are weaker than in maize. To investigate whether this was due to the differences in the Gβ protein, we expressed maize *ZmGB1* in *Arabidopsis*, driven by the native *AGB1* promoter. The *ZmGB1* transgene fully rescued the developmental and immune defects of *agb1* mutants (*SI Appendix*, Fig. S1), suggesting that Gβ function is conserved between maize and *Arabidopsis*, and that the contrasting immune phenotypes are not due to differences in the Gβ protein.

***Zmgb1* Lethality Can Be Suppressed.** The early lethality of $Zmgb1^{CR}$ plants precluded us from observing their meristem phenotypes. Autoimmune phenotypes are common for proteins that are "guardees," protected (or guarded) by RESISTANCE (R) proteins (32). Since *R* genes are highly polymorphic across accessions, we attempted to suppress $Zmgb1^{CR}$ autoimmunity by crossing viable heterozygotes to each of the 25 nested association mapping (NAM) maize diversity lines (33) and then screening for suppression in the F2s. Indeed, we found that the lethality of $Zmgb1^{CR}$ could be partially suppressed after crossing to a tropical maize line, CML103. The suppressed $Zmgb1^{CR}$ mutants were dwarfed with wider stems, similar to the maize *ct2* (*Gα*) mutants (Fig. 2*A*) (21), and some of the plants survived to flowering (Fig. 2*B*).

Consistent with this growth recovery, the induction of *PR1* and *PR5* immune marker genes was reduced in the suppressed $Zmgb1^{CR}$ mutants (*SI Appendix*, Fig. S2), confirming that autoimmunity was also suppressed. We took advantage of these lethality-suppressed $Zmgb1^{CR}$ mutants to study the development of their meristems. The mutants had significantly larger SAMs compared with WT sibs (Fig. 2 *C* and *D*) and fasciated IMs (Fig. 2*E*), indicating that *ZmGB1* controls both SAM and IM development in maize.

A Newly Identified Fasciated Ear Mutant, *fea*183*, Encodes a Viable Allele of *ZmGB1*. Concurrently, we identified a viable recessive allele of *Zmgb1* by map-based cloning of *fea*183*, a fasciated ear mutant from an ethyl methanesulfonate (EMS)-mutagenesis screen. *fea*183* mutants were semidwarf and had shorter, wider leaves with prominent lesions (Fig. 3*A*). They also had striking inflorescence defects, including fasciated ears and compact tassels (Fig. 3 *B* and *C* and *SI Appendix*, Fig. S3*A*), reminiscent of *ct2* mutants (21). We analyzed developing ear and tassel primordia using scanning electron microscopy (SEM) and found that their IMs were significantly enlarged (Fig. 3*B* and *SI Appendix*, Fig. S3*B*). In addition to IM defects, *fea*183* mutants had larger shoot apical meristems (Fig. 3 *D* and *E*). The mutants also had obvious cell death and up-regulation of *PR* genes, suggesting an autoimmune phenotype, albeit much weaker than that of $Zmgb1^{CR}$ mutants (*SI Appendix*, Fig. S3 *C* and *D*).

Bulked segregant analysis and map-based cloning delineated the *fea*183* mutation between 257.3 Mb and 258.9 Mb on chromosome 1 (Fig. 3*F* and *SI Appendix*, Fig. S4*A*). Whole-genome sequencing identified a single nonsynonymous mutation within this region, a G-to-A substitution in the fourth exon of *ZmGB1*, leading to a change in the amino acid 277 from aspartic acid to asparagine in 1 of the WD40 domains (*SI Appendix*, Fig. S4*B*). This residue is fully conserved across a wide range of species, including *Saccharomyces cerevisiae*, *Caenorhabditis elegans*, *Homo sapiens*, and *Arabidopsis*, implying its essential role in Gβ function (*SI Appendix*, Fig. S4*C*). We next confirmed that *fea*183* encoded an allele of *ZmGB1* by crossing with $Zmgb1^{CR}$ heterozygous plants. In the F1, approximately one-half of the plants had enlarged IMs and dwarfism, similar to *fea*183* mutants (Fig. 3 *G* and *H*), indicating a failure to complement and demonstrating that *FEA*183* encodes the maize Gβ subunit. Thus, we renamed *fea*183* as $Zmgb1^{fea*183}$.

We next asked how the $D^{277}N$ mutation affects $Zmgb1^{fea*183}$ function, by comparing it with human Gβ, HsGB1, and guided by a structure of the human G protein complex (34). The D^{277} residue in $Zmgb1^{fea*183}$ aligned to D^{254} in HsGB1 (34) (Fig. 4*A*), which lies at the interface of Gβ and Gγ (Fig. 4*B*). We thus asked whether this residue is required to form the heterotrimeric complex, using a yeast 3-hybrid (Y3H) experiment (35). We found that unlike the WT protein, the $Zmgb1^{fea*183}$ protein could not form a

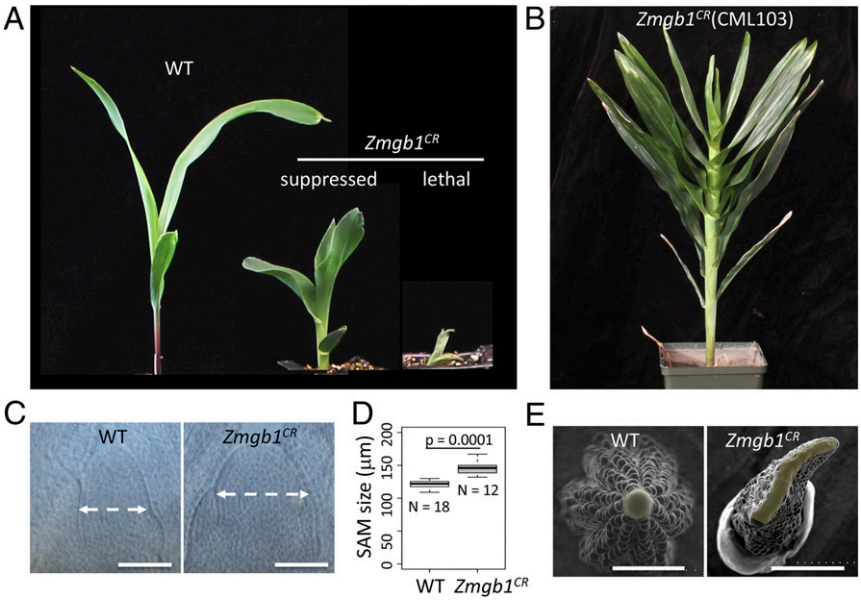

Fig. 2. The lethality of $Zmgb1^{CR}$ mutants was suppressed in the CML103 background. (*A*) F2 progeny of a cross between $Zmgb1^{CR}$ heterozygotes and CML103 segregates for lethal and suppressed phenotypes. The pictures are of 7-d-old maize seedlings. (*B*) The suppressed $Zmgb1^{CR}$ plants in the CML103 background grew to the adult stage. (*C* and *D*) $Zmgb1^{CR}$ mutants had enlarged SAMs (*C*), quantified in (*D*). $P = 0.0001$, Student's *t* test; $n = 18$ for WT and $n = 12$ for $Zmgb1^{CR}$. (*E*) Top-down view of WT and $Zmgb1^{CR}$ ear primordia in the SEM. IMs are shaded in yellow. (Scale bars: 100 μm in *C* and 1 mm in *E*.)

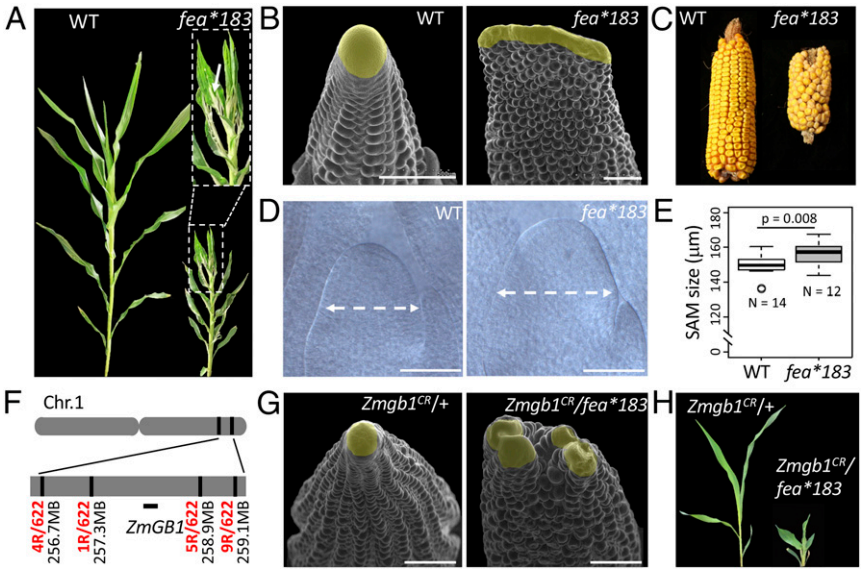

Fig. 3. Characterization and mapping of the *fea*183* mutant. (*A*) *fea*183* plants were semidwarf with upright leaves and lesions (*Inset*, dotted lines). The lesion part was arrowed. (*B*) SEM images showing that *fea*183* mutant ear primordia had enlarged IMs, shaded in yellow. (Scale bars: 500 μm.) (*C*) Representative mature cobs of WT and *fea*183* showing the fasciated ear phenotype. (*D*) Cleared SAM images of 12-d-old WT and *fea*183* mutants. (Scale bars: 100 μm.) (*E*) *fea*183* mutants had larger SAMs. $P = 0.008$, Student's *t* test; $n = 14$ for WT and $n = 12$ for *fea*183*. (*F*) Positional cloning of *fea*183* mutant identified *ZmGB1* as the candidate gene. The vertical lines indicate the position of markers used. The numbers of recombinants at each position are listed in red. (*G*) *fea*183* failed to complement $Zmgb1^{CR}$ in IM development. Shown are SEM images of ear primordia. (Scale bars: 500 μm.) (*H*) *fea*183* failed to complement $Zmgb1^{CR}$ seedling development. Pictures are of 2-wk-old seedlings.

complex with a maize Gγ subunit (ZmRGG2) and Gα/CT2, or with any of the XLG proteins (Fig. 4*C*), indicating that $Zmgb1^{fea*183}$ is unable to form a heterotrimeric complex and suggesting that it is a null allele. Consistent with this idea, we found that the SAM and IM phenotypes of $Zmgb1^{fea*183}$ mutants were indistinguishable from $Zmgb1^{fea*183}$/null $Zmgb1^{CR}$ plants (*SI Appendix*, Fig. S5).

ZmGB1 Functions in the CLAVATA Pathway. To further decipher the role of ZmGB1, we made double mutants using the $Zmgb1^{fea*183}$ allele with other meristem regulatory genes, including *fea2*, *ct2*, and *fea3* (13, 15, 21), and measured meristem size in segregating populations. The SAMs and ear IMs of *Zmgb1;fea2* double mutants were not obviously different from those of the *fea2* single mutant, indicating that *fea2* is epistatic to *Zmgb1* and suggesting that they act in a common pathway (Fig. 5 *A*–*C*). Similarly, IMs of *Zmgb1;ct2* double mutants were no more fasciated than either single mutant, suggesting that ZmGB1 and CT2/Gα function together in regulating IM development (Fig. 5*D*). However, vegetative SAMs of *Zmgb1;ct2* double mutants were more severely affected than the single mutant, presumably because CT2 acts redundantly with ZmXLGs during vegetative development (35) (Fig. 5 *E* and *F*). Finally, *Zmgb1;fea3* double

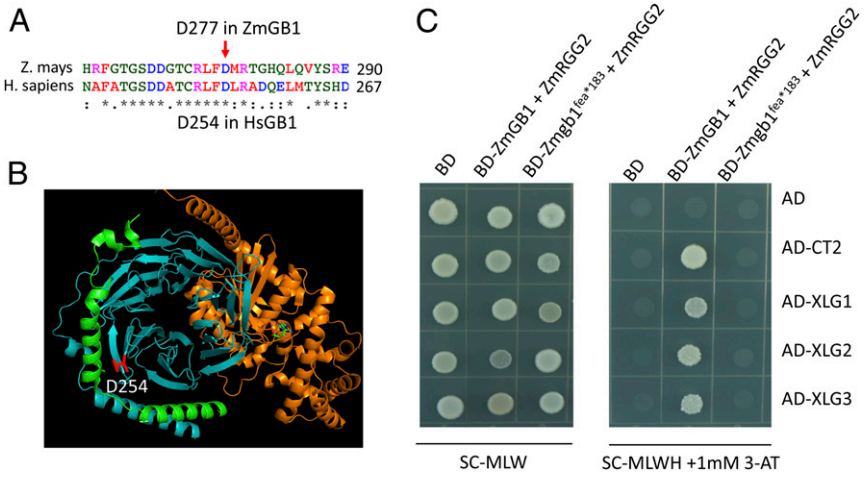

Fig. 4. $Zmgb1^{fea*183}$ failed to form a protein complex with Gα and Gγ subunits. (*A*) The D277 residue mutated in $Zmgb1^{fea*183}$ aligns to D254 in human HsGB1. (*B*) D254 highlighted in red in HsGB1 is located at the Gβ–Gγ interface. Viewed by PyMoL, with the Gα subunit in orange, the Gβ subunit in cyan, and the Gγ subunit in green. (*C*) ZmGB1 and the ZmRGG2 Gγ subunit formed complexes with Gα/CT2 or XLGs in a Y3H assay, while $Zmgb1^{fea*183}$ did not. ZmGB1 was fused with the BD domain and coexpressed with RGG2 using a pBridge construct (Clontech). Gα/CT2 or individual XLG proteins were fused with the AD domain in the pGADT7 vector. Yeast growth on synthetic complete-Met-Trp-Leu (SC-MLW) medium confirmed transformation and cell viability. Interactions were assayed on SC-Met-Trp-Leu-His (SC-MLWH) medium supplemented with 1 mM 3-AT.

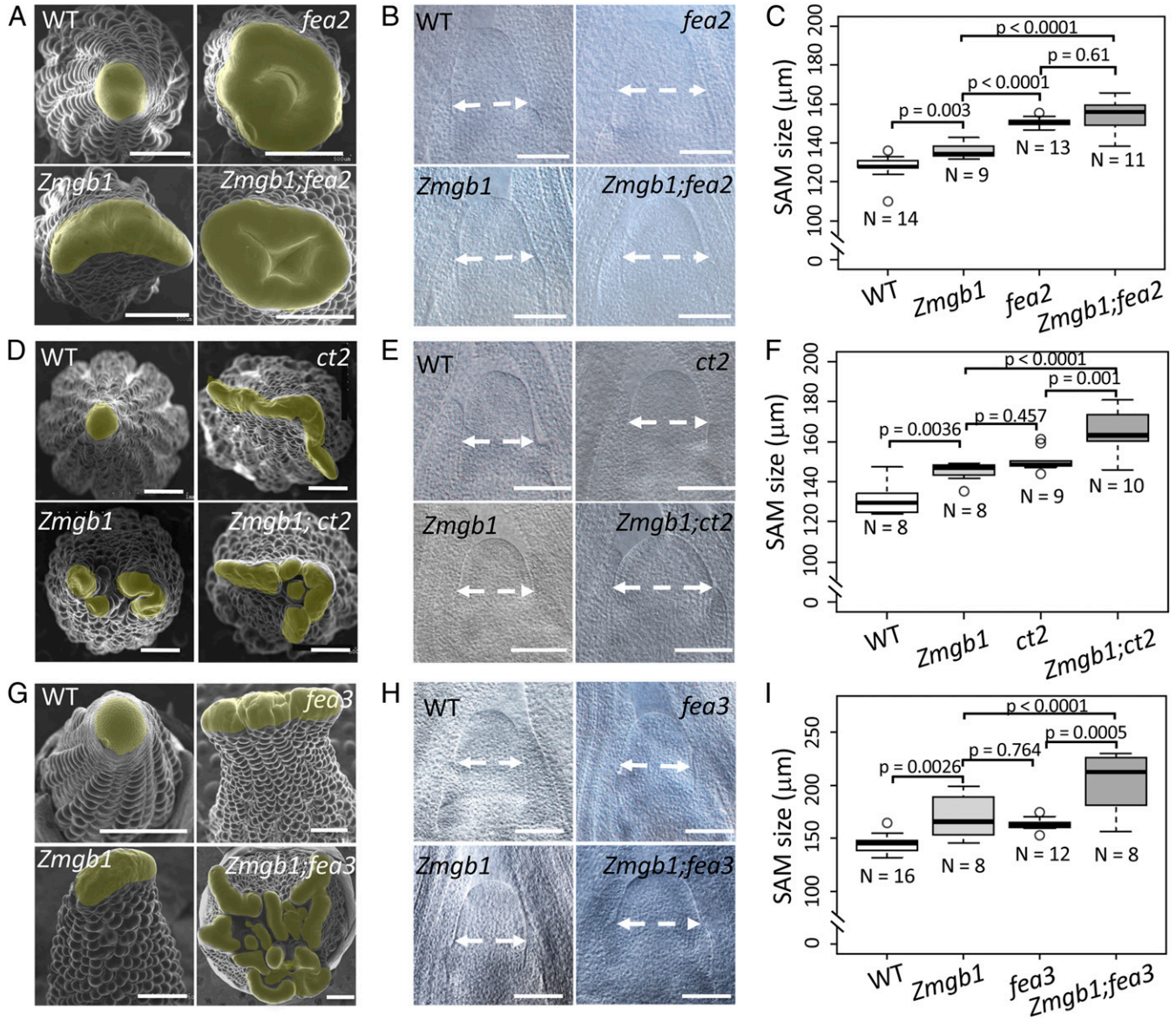

Fig. 5. ZmGB1 functions in a CLAVATA pathway. (*A*) SEM images of WT, *Zmgb1*, *fea2*, and *Zmgb1;fea2* ear primordia. The double mutants showed similar IMs as the *fea2* single mutant. (*B*) Representative SAM pictures from 16-d-old WT, *Zmgb1*, *fea2*, and *Zmgb1;fea2* plants. (*C*) SAM size quantification showed that the SAM size of the *Zmgb1;fea2* double mutants was indistinguishable from that of the *fea2* single mutants. (*D*) SEM images of WT, *Zmgb1*, *ct2*, and *Zmgb1;ct2* ear primordia. The double mutants showed similar IMs as the single mutants. (*E*) Representative SAM pictures of WT, *Zmgb1*, *ct2*, and *Zmgb1;ct2* plants. (*F*) SAM size was significantly larger in the *Zmgb1;ct2* double mutant compared with the single mutants. (*G*) SEM images of WT, *Zmgb1*, *fea3*, and *Zmgb1;fea3* ear primordia. The IMs were significantly larger in the double mutant compared with the single mutants. (*H*) Representative SAM pictures of 16-d-old WT, *Zmgb1*, *fea3*, and *Zmgb1;fea3* plants. (*I*) SAM size was significantly larger in the *Zmgb1;fea3* double mutant than in the single mutants. In *C*, *F*, and *I*, ANOVA analysis was performed with R. *P* values, mean values, and replicate numbers are indicated in the figures. (Scale bars: 500 μm for *A*, *D*, and *G*; 100 μm for *B*, *E*, and *H*.)

mutants had significantly larger SAMs and more strongly fasciated IMs than either single mutant (Fig. 5 *G*–*I*), indicating an additive genetic effect and demonstrating that *Zmgb1* and *fea3* act in different pathways in both SAM and IM regulation, in line with previous observations (36). In summary, our data suggest that ZmGB1 functions together with CT2/Gα in inflorescence development, downstream of the FEA2 CLAVATA receptor.

***ZmGB1* Associates with Maize Kernel Row Number.** Kernel row number (KRN) is an important agronomic trait that directly contributes to yield (15, 37, 38). Natural or induced variation in *FEA2* or *FEA3* is associated with KRN, and manipulation of *CT2* also enhances KRN (15, 35, 37). Therefore, we asked whether *ZmGB1* also associates with this yield trait by conducting a candidate gene association study using a maize association panel of 368 diverse inbred lines (39). Indeed, we found that 5 SNPs in the first and third exons of *ZmGB1* significantly associated with maize KRN (Fig. 6*A*). However, all of the SNPs were synonymous and did not change the ZmGB1 protein sequence, suggesting that the variation in KRN is due to changes in *ZmGB1* expression. These 5 KRN-associated SNPs can form 4 kinds of haplotypes among the 368 lines, 2 of which (Hap3 and Hap4) have significantly more kernel rows than the other 2 (Fig. 6*B*). For example, Hap4 has on average 1.5 and 2.5 more kernel rows compared with Hap2 and Hap1, respectively (Fig. 6*B*). However, the frequencies of favorable Hap3 and Hap4 in the association panel are only 2.17% and 4.07%, implying that the favorable *ZmGB1* alleles have not been selected during maize breeding. Therefore, our

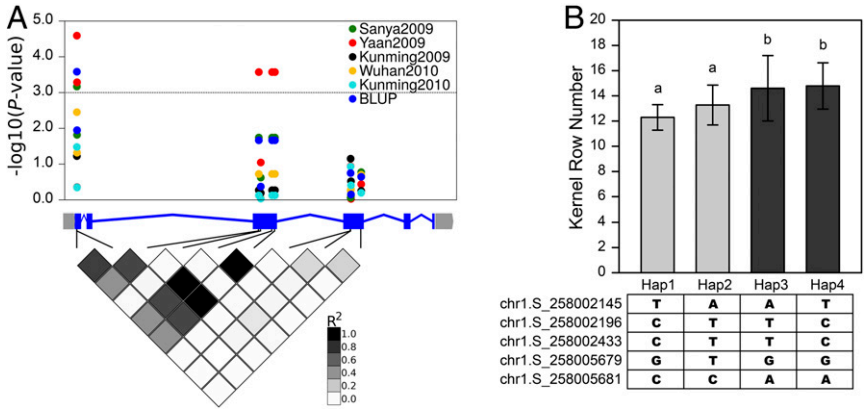

Fig. 6. Association analysis of *ZmGB1* with KRN. (*A*) The dots show multiple coding SNPs that associate positively with KRN over multiple environments, along with their best linear unbiased prediction (BLUP) data. A total of 368 diverse inbred lines were used in the association analysis using the MLM + Q model. Shaded diamonds below the gene model show the SNP linkage disequilibrium by pairwise R^2 values. (*B*) Haplotype analysis using the 5 KRN-associated SNPs and the KRN (BLUP) of these haplotypes in the association panel. Multiple comparisons $P < 0.05$. Chr1.s.number refers to the coordinate of maize chromosome 1 based on B73 V2 genome.

results suggest that natural variation in *ZmGB1* influences IM size and KRN, with the potential to benefit maize yields.

Discussion

Heterotrimeric G proteins are important signal transducers that control many biological processes across a wide range of species (17, 40). They also control many important agronomic traits in cereals (21, 28, 35, 41–44), and understanding G protein signaling requires a study of each subunit. Rice *Gβ* CRISPR null mutants undergo early developmental arrest and death, but the underlying mechanism was unclear (28, 29). Here we show that maize *Gβ* null alleles are also lethal, and that this is due to autoimmunity, not to specific developmental defects. We suppressed the *Gβ* lethal phenotype in the CML103 tropical maize genetic background and identified a viable EMS allele, allowing developmental analysis of *Gβ* meristems. Using the suppressed CRISPR null and the viable *Zmgb1*^{fea*183} alleles, we show that Gβ controls shoot meristem development. Our results suggest that Gβ interacts with different downstream effectors to function independently in immune and development signaling.

An important question is why only monocot *Gβ* mutants, such as in rice or maize, but not *Arabidopsis* mutants, develop autoimmunity. Intriguingly, the *Arabidopsis Gβ* mutant *agb1* has a reduced immune response, in contrast to the autoimmune phenotype in rice or maize (24, 25). Expression of maize *Gβ* fully complemented the immune defects of *Arabidopsis agb1* mutants (*SI Appendix*, Fig. S1), suggesting that Gβ protein function is conserved, and that the contrasting phenotypes are probably due to differences in immune signaling pathways.

Plants have a 2-tiered immune system. First, pathogen-associated molecular pattern (PAMP) receptors recognize conserved microbial elicitors and induce pattern-triggered immunity (PTI) (45–47). To overcome PTI, pathogens have evolved effectors that they secrete into plant cells to interfere with PAMP signaling, and in turn, plants evolved *R* genes to activate the stronger effector-triggered immunity (ETI), which often results in programmed cell death (48–51). Some R proteins guard native plant proteins, known as "guardees," that are targeted by pathogen effectors. Thus, mutation of a guardee may mimic the presence of a pathogen and activate the guarding R protein, resulting in an autoimmune phenotype (52). Therefore, it is reasonable to speculate that grass Gβ proteins function as immune guardees. Supporting this hypothesis, Gβ has 7 WD-40 domains and forms a propeller structure, similar to some other effector targets (53).

Our hypothesis explains why the immune phenotypes of *Zmgb1*^{fea*183} mutants are weaker, because presumably this allele accumulates some (albeit mutant) Gβ protein that can still interact with a hypothetical guard R protein but is recognized as abnormal, initiating a partial autoimmune response. *R* genes are highly polymorphic across accessions, and our results suggest that Gβ is guarded in the monocots rice and maize, but not *Arabidopsis* (53). To test this hypothesis, further studies are needed to identify the gene(s) responsible for the suppression of *Zmgb1* lethality in CML103.

Our genetic analyses suggest that ZmGB1 works in a common pathway with FEA2 and CT2/Gα but independent of FEA3. *fea2* was epistatic to both *ct2* (*Gα*) and *Zmgb1* in IM fasciation, suggesting that both G protein subunits function together downstream of the FEA2 receptor. However, *ct2*/*Gα* and *Zmgb1* phenotypes were additive in the SAM, which could be explained by redundancy with the noncanonical Gα proteins, or XLGs, in the SAM (35). However, *Zmxlg* triple mutants are also lethal (35), preventing us from making higher-order mutants in maize. Identification of a viable genetic background for *Gα* higher-order mutants would help address this question.

Geneticists and breeders have used quantitative trait locus (QTL) and genome-wide association analyses to identify genes involved in yield traits. Several yield QTL that correspond to heterotrimeric G proteins or CLV-WUS genes have been cloned in rice, maize, and tomato (38, 42, 54–56). For example, *FEA2* is a QTL responsible for variation in maize KRN (37), and a rice *Gγ* gene, *GS3*, is a QTL for grain length, weight, and thickness (44), while another rice *Gγ* gene, *DEP1*, is a QTL for rice grain yield and nitrogen use efficiency (42, 43). These studies indicate that G proteins and other meristem regulators have the potential to benefit yield traits. In this study, we found that *ZmGB1* also associated significantly with KRN under multiple environments, suggesting that it also contributes to quantitative variation in KRN. In rice, overexpression of *RGB1* enhances tolerance to biotic and abiotic stresses (57, 58), but grain size is reduced (41), suggesting that more subtle modulation of *ZmGB1* expression is needed to optimize yield (15, 37, 59).

Improving crop productivity involves selection of favorable architecture and development alleles. Despite these striking innovations, crops are constantly under attack from pathogens. However, turning on defense signaling often causes reductions in growth and yield (60, 61). This defense–growth trade-off results from the intertwining of defense signaling with physiological networks regulating plant fitness (60). Therefore, an understanding of developmental and immune signaling cross-talk is critical to provide basic knowledge to maximize productivity. Our study shows that *ZmGB1* is a critical regulator in both meristem development and immunity; therefore, this gene has the potential to optimize defense–development trade-offs to improve agronomic production.

Materials and Methods

The *Zmgb1*^{CR} alleles were created using CRISPR/Cas9, and the *Zmgb1*^{fea*183} allele was obtained from an EMS mutagenesis screen using seed stocks provided by Gerald Neuffer. Complete details regarding materials, experimental methods, and data analyses are provided in *SI Appendix*. All data are contained in the paper and *SI Appendix*. All of the data and materials will be available on request from the corresponding author.

ACKNOWLEDGMENTS. We thank Dr. Gerald Neuffer, and the Maize Genetics Stock Center for the *Zmgb1*^{fea*183} EMS mutant. We thank Dr. Geert De Jaeger; VIB-UGent Center for Plant Systems Biology for providing the YFP-SBP sequence. Funding for this work was provided by the US Department of Agriculture, National Institute of Food and Agriculture (Agriculture and Food Research Initiative Competitive Grants 2017-06299 and 2015-06319, to D.J.), the Next-Generation BioGreen 21 Program System & Synthetic Agro-biotech Center (Grant PJ01322602) from the Rural Development Administration, Republic of Korea (to D.J.), and the NSF (Grant ISO-1936492, to B.Y.). Q.W. was supported by the National Science and Technology Major Project for Development of Transgenic Organisms (2019ZX08010004), National Natural Science Foundation of China (31601822), and Innovation Program of Chinese Academy of Agricultural Sciences. F.X. was supported by the Taishan Scholars of Shandong Province (Grant tsqn201812018), Shandong University (Qilu Scholarship 61200089963066), and the Human Frontier Science Program (Long-Term Fellowship LT000227/2016). B.I.J. was supported by the Basic Science Research Program through the National Research Foundation of Korea, funded by the Ministry of Education, Science and Technology (NRF-2018R1A4A1025158).

1. Q. Wu, F. Xu, D. Jackson, All together now, a magical mystery tour of the maize shoot meristem. *Curr. Opin. Plant Biol.* **45**, 26–35 (2018).
2. S. E. Clark, R. W. Williams, E. M. Meyerowitz, The CLAVATA1 gene encodes a putative receptor kinase that controls shoot and floral meristem size in Arabidopsis. *Cell* **89**, 575–585 (1997).
3. J. C. Fletcher, U. Brand, M. P. Running, R. Simon, E. M. Meyerowitz, Signaling of cell fate decisions by CLAVATA3 in Arabidopsis shoot meristems. *Science* **283**, 1911–1914 (1999).
4. H. Schoof *et al*., The stem cell population of Arabidopsis shoot meristems in maintained by a regulatory loop between the CLAVATA and WUSCHEL genes. *Cell* **100**, 635–644 (2000).
5. R. K. Yadav *et al*., WUSCHEL protein movement mediates stem cell homeostasis in the Arabidopsis shoot apex. *Genes Dev.* **25**, 2025–2030 (2011).
6. G. Daum, A. Medzihradszky, T. Suzaki, J. U. Lohmann, A mechanistic framework for noncell autonomous stem cell induction in Arabidopsis. *Proc. Natl. Acad. Sci. U.S.A.* **111**, 14619–14624 (2014).
7. M. Perales *et al*., Threshold-dependent transcriptional discrimination underlies stem cell homeostasis. *Proc. Natl. Acad. Sci. U.S.A.* **113**, E6298–E6306 (2016).
8. U. Brand, J. C. Fletcher, M. Hobe, E. M. Meyerowitz, R. Simon, Dependence of stem cell fate in Arabidopsis on a feedback loop regulated by CLV3 activity. *Science* **289**, 617–619 (2000).
9. M. Ogawa, H. Shinohara, Y. Sakagami, Y. Matsubayashi, Arabidopsis CLV3 peptide directly binds CLV1 ectodomain. *Science* **319**, 294 (2008).
10. S. Jeong, A. E. Trotochaud, S. E. Clark, The Arabidopsis CLAVATA2 gene encodes a receptor-like protein required for the stability of the CLAVATA1 receptor-like kinase. *Plant Cell* **11**, 1925–1934 (1999).
11. R. Müller, A. Bleckmann, R. Simon, The receptor kinase CORYNE of Arabidopsis transmits the stem cell-limiting signal CLAVATA3 independently of CLAVATA1. *Plant Cell* **20**, 934–946 (2008).
12. F. Taguchi-Shiobara, Z. Yuan, S. Hake, D. Jackson, The fasciated ear2 gene encodes a leucine-rich repeat receptor-like protein that regulates shoot meristem proliferation in maize. *Genes Dev.* **15**, 2755–2766 (2001).
13. P. Bommert *et al*., Thick tassel dwarf1 encodes a putative maize ortholog of the Arabidopsis CLAVATA1 leucine-rich repeat receptor-like kinase. *Development* **132**, 1235–1245 (2005).
14. D. M. Goad, C. Zhu, E. A. Kellogg, Comprehensive identification and clustering of CLV3/ESR-related (CLE) genes in plants finds groups with potentially shared function. *New Phytol.* **216**, 605–616 (2017).
15. B. I. Je *et al*., Signaling from maize organ primordia via FASCIATED EAR3 regulates stem cell proliferation and yield traits. *Nat. Genet.* **48**, 785–791 (2016).
16. D. Rodriguez-Leal *et al*., Evolution of buffering in a genetic circuit controlling plant stem cell proliferation. *Nat. Genet.* **51**, 786–792 (2019).
17. I. Gomes *et al*., G protein-coupled receptor heteromers. *Annu. Rev. Pharmacol. Toxicol.* **56**, 403–425 (2016).
18. J. C. Jones, B. R. S. Temple, A. M. Jones, H. G. Dohlman, Functional reconstitution of an atypical G protein heterotrimer and regulator of G protein signaling protein (RGS1) from Arabidopsis thaliana. *J. Biol. Chem.* **286**, 13143–13150 (2011).
19. D. Urano, A. M. Jones, Round up the usual suspects: A comment on nonexistent plant GPCRs. *Plant Physiol.* **161**, 1097–1102 (2013).
20. B. Taddese *et al*., Do plants contain g protein-coupled receptors? *Plant Physiol.* **164**, 287–307 (2014).
21. P. Bommert, B. I. Je, A. Goldshmidt, D. Jackson, The maize Gα gene COMPACT PLANT2 functions in CLAVATA signalling to control shoot meristem size. *Nature* **502**, 555–558 (2013).
22. S. R. Choudhury, S. Pandey, Specific subunits of heterotrimeric G proteins play important roles during nodulation in soybean. *Plant Physiol.* **162**, 522–533 (2013).
23. T. Ishida *et al*., Heterotrimeric G proteins control stem cell proliferation through CLAVATA signaling in Arabidopsis. *EMBO Rep.* **15**, 1202–1209 (2014).
24. X. Liang *et al*., Arabidopsis heterotrimeric G proteins regulate immunity by directly coupling to the FLS2 receptor. *eLife* **5**, e13568 (2016).
25. J. Liu *et al*., Heterotrimeric G proteins serve as a converging point in plant defense signaling activated by multiple receptor-like kinases. *Plant Physiol.* **161**, 2146–2158 (2013).
26. Y. Utsunomiya *et al*., Suppression of the rice heterotrimeric G protein β-subunit gene, RGB1, causes dwarfism and browning of internodes and lamina joint regions. *Plant J.* **67**, 907–916 (2011).
27. D. Urano, R. Leong, T. Y. Wu, A. M. Jones, Quantitative morphological phenomics of rice G protein mutants portend autoimmunity. *Dev. Biol.*, 10.1016/j.ydbio.2019.09.007 (2019).
28. S. Sun *et al*., A G-protein pathway determines grain size in rice. *Nat. Commun.* **9**, 851 (2018).
29. Y. Gao *et al*., The heterotrimeric G protein β subunit RGB1 is required for seedling formation in rice. *Rice (N. Y.)* **12**, 53 (2019).
30. D. Urano *et al*., Saltational evolution of the heterotrimeric G protein signaling mechanisms in the plant kingdom. *Sci. Signal.* **9**, ra93 (2016).
31. C. Kato *et al*., Characterization of heterotrimeric G protein complexes in rice plasma membrane. *Plant J.* **38**, 320–331 (2004).
32. R. A. van der Hoorn, S. Kamoun, From guard to decoy: A new model for perception of plant pathogen effectors. *Plant Cell* **20**, 2009–2017 (2008).
33. M. D. McMullen *et al*., Genetic properties of the maize nested association mapping population. *Science* **325**, 737–740 (2009).
34. S. Maeda *et al*., Development of an antibody fragment that stabilizes GPCR/G-protein complexes. *Nat. Commun.* **9**, 3712 (2018).
35. Q. Wu, M. Regan, H. Furukawa, D. Jackson, Role of heterotrimeric Gα proteins in maize development and enhancement of agronomic traits. *PLoS Genet.* **14**, e1007374 (2018).
36. B. I. Je *et al*., The CLAVATA receptor FASCIATED EAR2 responds to distinct CLE peptides by signaling through two downstream effectors. *eLife* **7**, e35673 (2018).
37. P. Bommert, N. S. Nagasawa, D. Jackson, Quantitative variation in maize kernel row number is controlled by the FASCIATED EAR2 locus. *Nat. Genet.* **45**, 334–337 (2013).
38. L. Liu *et al*., KRN4 controls quantitative variation in maize kernel row number. *PLoS Genet.* **11**, e1005670 (2015).
39. X. H. Yang *et al*., Characterization of a global germplasm collection and its potential utilization for analysis of complex quantitative traits in maize. *Mol. Breed.* **28**, 511–526 (2011).
40. D. Urano, A. M. Jones, Heterotrimeric G protein-coupled signaling in plants. *Annu. Rev. Plant Biol.* **65**, 365–384 (2014).
41. Q. Liu *et al*., G-protein βγ subunits determine grain size through interaction with MADS-domain transcription factors in rice. *Nat. Commun.* **9**, 852 (2018).
42. X. Huang *et al*., Natural variation at the DEP1 locus enhances grain yield in rice. *Nat. Genet.* **41**, 494–497 (2009).
43. H. Sun *et al*., Heterotrimeric G proteins regulate nitrogen-use efficiency in rice. *Nat. Genet.* **46**, 652–656 (2014).
44. C. Fan *et al*., GS3, a major QTL for grain length and weight and minor QTL for grain width and thickness in rice, encodes a putative transmembrane protein. *Theor. Appl. Genet.* **112**, 1164–1171 (2006).
45. T. Boller, G. Felix, A renaissance of elicitors: Perception of microbe-associated molecular patterns and danger signals by pattern-recognition receptors. *Annu. Rev. Plant Biol.* **60**, 379–406 (2009).
46. L. Gómez-Gómez, T. Boller, FLS2: An LRR receptor-like kinase involved in the perception of the bacterial elicitor flagellin in Arabidopsis. *Mol. Cell* **5**, 1003–1011 (2000).
47. J. Monaghan, C. Zipfel, Plant pattern recognition receptor complexes at the plasma membrane. *Curr. Opin. Plant Biol.* **15**, 349–357 (2012).
48. A. F. Bent, D. Mackey, Elicitors, effectors, and R genes: The new paradigm and a lifetime supply of questions. *Annu. Rev. Phytopathol.* **45**, 399–436 (2007).
49. J. L. Caplan, P. Mamillapalli, T. M. Burch-Smith, K. Czymmek, S. P. Dinesh-Kumar, Chloroplastic protein NRIP1 mediates innate immune receptor recognition of a viral effector. *Cell* **132**, 449–462 (2008).
50. S. T. Chisholm, G. Coaker, B. Day, B. J. Staskawicz, Host-microbe interactions: Shaping the evolution of the plant immune response. *Cell* **124**, 803–814 (2006).
51. J. D. Jones, J. L. Dangl, The plant immune system. *Nature* **444**, 323–329 (2006).
52. J. Chakraborty, P. Ghosh, S. Das, Autoimmunity in plants. *Planta* **248**, 751–767 (2018).
53. P. F. Sarris, V. Cevik, G. Dagdas, J. D. G. Jones, K. V. Krasileva, Comparative analysis of plant immune receptor architectures uncovers host proteins likely targeted by pathogens. *BMC Biol.* **14**, 8 (2016).
54. Y. Jiao *et al*., Regulation of OsSPL14 by OsmiR156 defines ideal plant architecture in rice. *Nat. Genet.* **42**, 541–544 (2010).
55. J. Liu *et al*., GW5 acts in the brassinosteroid signalling pathway to regulate grain width and weight in rice. *Nat. Plants* **3**, 17043 (2017).
56. K. Miura *et al*., OsSPL14 promotes panicle branching and higher grain productivity in rice. *Nat. Genet.* **42**, 545–549 (2010).
57. S. Biswas, M. N. Islam, S. Sarker, N. Tuteja, Z. I. Seraj, Overexpression of heterotrimeric G protein beta subunit gene (OsRGB1) confers both heat and salinity stress tolerance in rice. *Plant Physiol. Biochem.* **144**, 334–344 (2019).
58. D. M. Swain *et al*., Function of heterotrimeric G-protein γ subunit RGG1 in providing salinity stress tolerance in rice by elevating detoxification of ROS. *Planta* **245**, 367–383 (2017).
59. D. Rodríguez-Leal, Z. H. Lemmon, J. Man, M. E. Bartlett, Z. B. Lippman, Engineering quantitative trait variation for crop improvement by genome editing. *Cell* **171**, 470–480.e8 (2017).
60. T. L. Karasov, E. Chae, J. J. Herman, J. Bergelson, Mechanisms to mitigate the trade-off between growth and defense. *Plant Cell* **29**, 666–680 (2017).
61. B. Huot, J. Yao, B. L. Montgomery, S. Y. He, Growth-defense tradeoffs in plants: A balancing act to optimize fitness. *Mol. Plant* **7**, 1267–1287 (2014).